

## Valence Band Emission Spectra of Iron, Cobalt, and Nickel\*

D. H. TOMBOULIAN AND D. E. BEDO  
*Cornell University, Ithaca, New York*

(Received August 25, 1960)

The paper presents results on the shapes of the  $M_{2,3}$  emission bands (valence  $\rightarrow 3p$ ) of Fe, Co, and Ni. The relative intensity distributions were arrived at by removing the underlying background contribution in accordance with the predictions made available from recent investigations dealing with the behavior of the soft x-ray bremsstrahlung intensity. In the spectrum of Fe the peak of the composite  $M_{2,3}$  band falls at 51.3 ev. The peaks in the Co and Ni spectra are located at 57.8 ev and 64.8 ev, respectively. The high-energy limits are estimated to fall at 56.5 ev, 61.4 ev, and 68.9 ev for Fe, Co, and Ni, respectively. The over-all composite bandwidths in ev in the order of metals just cited are found to be: 14.5, 10.8, and 9.3. These estimates include the low-energy tail belonging to the individual  $M_3$  spectral bands. An attempt was made to resolve the Fe  $M_{2,3}$  complex band into individual  $M_2$  and  $M_3$  bands. In this process the inner levels were regarded as sharp, but the influence of Auger reorganization upon the relative band intensities was taken into account. For Fe, this process gives an individual bandwidth of 8.0 ev. The results of the present observations are compared with other determinations of band contours. The various measurements are in agreement as to the location of the peak energy but there are differences in the intensity profiles and bandwidths.

## INTRODUCTION

IN an earlier investigation<sup>1</sup> dealing with the copper  $M_{2,3}$  emission band, it was pointed out that the experimental determination of the characteristic emission band shape was dependent sensitively on the procedure followed in removing the background radiation. In the case of copper, information concerning the background was derived from an examination of exposures taken with other neighboring elements (Cr and Mn) as target materials. In sorting out the background, it was assumed that the continuous spectrum emitted by these metals under standardized values of the target current and potential had nearly the same shape, the absolute intensity in each case being governed by the exposure time and the atomic number. In practice, the observed background may be distorted by impurity bands and is modified by absorption in the surface of the grating, so that in treating the record it is not always possible to differentiate between the unwanted features and those that are characteristic of the valence band.

Recent investigations<sup>2</sup> of the soft x-ray continuum over the 80 Å to 180 Å region indicate that the relative power radiated per unit wavelength band varies as  $1/\lambda^\alpha$ . The value of  $\alpha$  is found to depend upon the atomic number of the metallic target and upon the target voltage. For target voltages lying in the 1–3 kv range and for a wide range in the atomic number of the target materials, the values of  $\alpha$  are observed to lie between 1.9 and 3.0. For the three metals (Fe, Co, Ni) of the iron group, a careful study of the intensity distribution of the bremsstrahlung produced by 3-kev electrons shows that a good fit is obtained for values of  $\alpha$  which fall between 2.3 and 2.4.

Since the wavelength dependence of the bremsstrahlung intensity may now be considered as known, it is no longer necessary to rely on information deduced from exposures obtained with neighboring elements. Instead it becomes possible to predict the expected shape of the continuous spectrum underlying the characteristic emission band of the metal in question. It is the purpose of this paper to present results on the shapes of the  $M_{2,3}$  valence bands of Fe, Co, and Ni as derived from heretofore unpublished measurements which have now been reduced by removing the background contribution in accordance with the scheme just mentioned.

## EXPERIMENTAL

For a discussion of the experimental arrangement and general procedures, the reader should consult the article on copper<sup>1</sup> and references contained therein. Comments relevant to the present work are confined primarily to the technique used in depositing the target layer. The evaporation of Fe, Co, and Ni involves the problem of alloying with the tungsten filament used as a heater. Because these metals are soluble in tungsten, it is desirable to distribute the charge to be evaporated so that only a limited amount of the molten metal is in contact with a given length of the filament. Thus the concentration of the metal in the metal-tungsten alloy is kept to a low level. Otherwise, the evaporator disintegrates before adequate evaporation rates are reached, since the melting point of the metal-tungsten alloy is reduced with an increase in the amount of metal dissolved. In practice, the evaporator was made by twisting together two 20-mil tungsten wires with a thinner (5–10 mil) wire of the metal and subsequently supporting the three stranded unit in a manner which prevented the collapse of the alloyed tungsten filament.

In obtaining records, freshly deposited target layers were bombarded for about fifteen minutes before recoating. Filaments of the type described were used for

\* This research was supported by the Office of Ordnance Research, U. S. Army.

<sup>1</sup> D. E. Bedo and D. H. Tomboulia, *Phys. Rev.* **113**, 464 (1959).

<sup>2</sup> T. J. Peterson and D. H. Tomboulia, *Bull. Am. Phys. Soc.* **4**, 419 (1959).

a dozen or more evaporations. The dispersed radiation was detected photographically. The source was operated at a pressure of about  $1 \times 10^{-6}$  mm of Hg, while the power input to the target was 300 watts (100 ma at 3000 v). Three-hour exposures yielded a satisfactory recording of the spectrum.

#### TREATMENT OF OBSERVATIONS

The total relative intensity (continuum plus characteristic) was obtained by photometric reduction of the spectrograms. Figure 1 shows a typical plot of the overall intensity distribution as a function of wavelength  $\lambda$ . The graph displays the characteristic  $M_{2,3}$  band of iron superimposed on the continuum. The expected behavior of the underlying continuum over the relevant spectral domain was determined by the application of the  $1/\lambda^{2.4}$  relation. In doing so the order response of the grating was taken into account. The predetermined shape was observed to agree with that of the observed total intensity (solid curve) at wavelengths in excess of 295 Å. At shorter wavelengths the contribution arising from the bremsstrahlung is indicated by the dotted curve. A similar method of sorting out of the continuum was carried out in the case of Co and Ni. In all instances the intensity of the characteristic band was comparable to that of the continuum.

Besides the background there are other factors which may give rise to a modification of the shape of the emission band. For instance, the intensity of the radiation is modified by absorption in the surface layers of the grating. Such an absorption appears over the wavelength interval extending from 115 Å to 118 Å. Depending on the exposure time, it is occasionally observed in the second order. The spectrogram may also be contaminated by the  $K_{\alpha}$  band ( $\lambda_{\text{peak}} = 44.5$  Å) of carbon. This band can appear in higher orders with gradually diminishing intensities. In the second order (at  $\lambda = 89$  Å) the peak intensity is 35% of that found in the first order; the corresponding percentages at the third ( $\lambda = 133.5$  Å) and fourth ( $\lambda = 178$  Å) order bands are 9% and 3%. For the Fe, Co, Ni bands studied here, contamination of the spectrum by C  $K_{\alpha}$  bands is not significant. If present at all, the sixth and fifth orders would modify the Fe and Co bands in the region of the tail. The fourth order falls on the short-wavelength side of the emission edge and is not expected to alter the shape of the band studied.

The effect of the grating absorption needs to be considered only in connection with the Fe spectrum, since the second order of this feature falls on the short-wavelength side of the peak in the Fe emission band. Observation indicates that the distortion produced in this case is not significant.

For a discussion of modifications brought about by the spectral window and by self-absorption in the target layer, the reader is referred to the paper listed in reference 1.

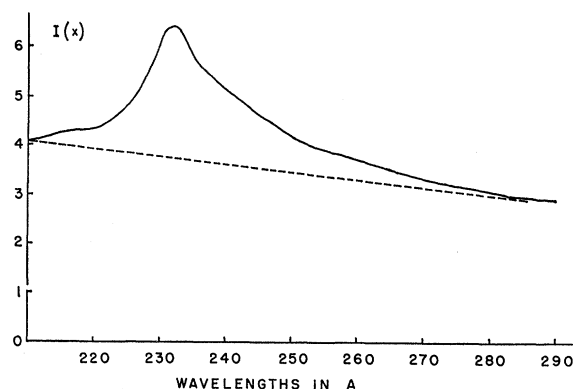


FIG. 1. A microphotometer record for the iron  $M_{2,3}$  emission band. The ordinate represents the total relative intensity of characteristic band and continuum. The contribution coming from the latter is indicated by the dashed line.

#### RESULTS

After removal of the contribution from the continuum, the measurements on the composite bands were converted so as to obtain the quantity  $I(E)/\nu^2$ . The latter represents<sup>3</sup> the relative intensity distribution divided by the square of the radiated frequency  $\nu$ . The spectral distribution  $I(E)$  is derived from the initial measurement  $I(x)$  which describes the intensity distribution as a function of position  $x$  along the Rowland circle. The conversion takes into account the instrumental dispersion and the connection between the spectral position  $x$  and  $E$  the energy of the emitted photon. The quantity  $I(E)/\nu^2$  is proportional to the product of the density of states function  $N(E)$  and average value of  $|M_{ik}|^2$ , the square of the matrix element between a bound state  $i$  and a valence state  $k$ . The calculated results for each metal are presented in Table I. In each case the results are normalized at the peak of the characteristic  $M_{2,3}$  band.

The measurements represent a superposition of the individual  $M_2$  (valence  $\rightarrow 3p_1$ ) and  $M_3$  (valence  $\rightarrow 3p_1$ ) emission bands. In the spectrum of iron the peak of the composite spectrum falls at  $E = 51.3$  eV. The peaks in the cobalt and nickel spectra are located at  $E = 57.8$  eV and at  $E = 64.8$  eV, respectively. The high-energy limits are estimated to fall at 56.5 eV, 61.4 eV, and 68.9 eV for iron, cobalt, and nickel, respectively. In all three cases the intensity drops slowly at the high-energy region of the band, and it is quite certain that the limits specified above do not correspond to the  $M_2$  emission edge, since satellite structure seems to be present.

At the low-energy end the band intensities drop to zero at 42.0 eV, 50.6 eV, and at 59.6 eV for the three metals in question. Thus the over-all widths in eV of the  $M_{2,3}$  composite bands, respectively, for iron, cobalt, and nickel are 14.5, 10.8, and 9.3. These estimates include the contribution of the low-energy tail belonging to

<sup>3</sup> D. H. Tomboulis, *Handbuch der Physik* (Springer-Verlag, Berlin, 1957), Vol. 30, p. 246.

TABLE I. Data on the  $M_{2,3}$  valence band emission spectra of iron, cobalt, and nickel. Values of the relative intensity distribution divided by the square of the radiated frequency are listed as a function of the photon energy  $E$  expressed in ev. The latter was obtained from the radiated wavelength with the help of  $E = 12397.43/\lambda$ , where  $\lambda$  is expressed in angstroms.

Iron		Cobalt		Nickel	
$E$ (ev)	$I(E)/\nu^2$	$E$ (ev)	$I(E)/\nu^2$	$E$ (ev)	$I(E)/\nu^2$
56.5	0.0	61.4	0.0	68.9	0.0
55.8	1.93	61.1	3.13	68.5	1.03
55.3	4.71	60.8	5.74	68.1	3.16
55.1	5.73	60.5	5.86	67.7	6.43
54.8	6.90	60.2	7.25	67.4	15.3
54.6	7.64	59.9	9.37	67.0	18.5
54.4	8.55	59.6	13.6	66.7	27.5
54.1	9.80	59.3	22.1	66.3	35.7
53.9	11.7	59.0	26.7	65.3	45.9
53.7	14.3	58.8	42.8	65.8	49.8
53.4	18.1	58.5	68.6	65.6	56.1
53.2	21.5	58.2	88.9	65.4	74.2
53.0	26.4	57.8	100.0	65.3	82.7
52.7	31.1	57.7	98.4	65.1	92.5
52.5	36.0	57.1	82.7	64.8	100.0
52.3	43.8	56.6	64.4	64.6	98.4
52.2	53.6	56.1	54.6	64.2	88.5
52.1	60.6	55.6	48.9	63.9	81.0
52.0	63.2	55.1	43.2	63.6	67.9
51.9	67.0	54.6	35.4	63.3	59.7
51.8	71.4	54.1	31.9	62.9	44.6
51.6	83.4	53.7	25.8	62.6	33.5
51.4	92.9	53.2	20.5	62.3	27.2
51.3	100.0	52.8	14.8	62.0	19.2
51.2	96.3	52.3	8.73	61.7	17.0
50.8	86.5	51.9	6.71	61.4	10.8
50.6	81.4	51.4	4.60	61.1	8.82
50.4	76.9	51.0	2.38	60.8	6.85
50.0	68.6	50.6	0.0	60.5	2.69
49.6	63.8			60.2	1.63
49.2	58.4			59.9	0.55
48.8	50.4			59.6	0.0
48.4	45.1				
48.1	37.6				
47.7	36.0				
47.3	32.1				
47.0	29.8				
46.6	27.8				
46.3	25.0				
45.9	23.3				
45.1	16.5				
44.3	11.5				
43.5	6.71				
42.8	3.59				
42.0	0.0				

the individual  $M_3$  band. Plots of the  $M_{2,3}$  emission bands are shown in Figs. 2-4.

A diffuseness over the region of high energies beyond the peak arises from the superposition of the individual  $M_2$  and  $M_3$  bands. Even the individual  $M_2$  or  $M_3$  spectra would be subject to a widening of the edge owing to the widths of the  $3p_{3/2}$  or  $3p_{1/2}$  state. By a roundabout manner one may make a crude estimate of the width of these states. Considering measurements involving  $L_3$  levels<sup>4</sup> and also the width of the  $L_3 \rightarrow M_{4,5}$  radiative transition in germanium<sup>5</sup> an upper limit to the width of the  $p$  states may be set at 0.2 ev. In addition, it is quite

likely that satellite structure modifies the shape of the individual emission bands at the high-energy limit.

Some insight regarding the shape of the component  $M_2$  and  $M_3$  bands might be gained if the observed emission intensity contour could be decomposed. In attempting such a resolution, it is necessary to consider the level density distribution of the individual  $M_2$  and  $M_3$  bands, the  $(M_2-M_3)$  energy interval, and the actual intensity relation between the component bands. In the present attempt, we shall regard the inner levels to be sharp but will take into account the influence of the Auger reorganization upon the relative intensities of the two bands.

In the emission process of interest here, photons are emitted when a vacancy in an  $M$  subshell of an atom is destroyed by an electron transition from the valence band. The ionization in the inner state is initially brought about by electron impact. To formulate an expression for the desired intensity ratio, let  $n_a$  denote the time rate at which atoms become ionized in an inner state  $a$  by some excitation process such as electron impact, photon irradiation, Auger process,  $K$  capture, or  $\gamma$ -ray conversion. Under equilibrium conditions,  $n_a$  will also represent the number of atoms/sec in which the vacancy is destroyed by all possible transitions with or without radiation from the state  $a$  into states  $i$  of lower energy.

The number of photons emitted per second corresponding to transitions from an initial level  $a$  to a final level  $k$  can be written as

$$n_{a \rightarrow k} = n_a (P_{a \rightarrow k}^R / P_a),$$

where  $P_{a \rightarrow k}^R$  is the transition rate for the radiative process in which the atom jumps from a high-energy state  $a$  to a lower energy state  $k$  and where  $P_a$  is the total transition probability per second for all processes which give rise to the decay of the initial state  $a$ , i.e.,

$$P_a = \sum_i P_{a \rightarrow i}.$$

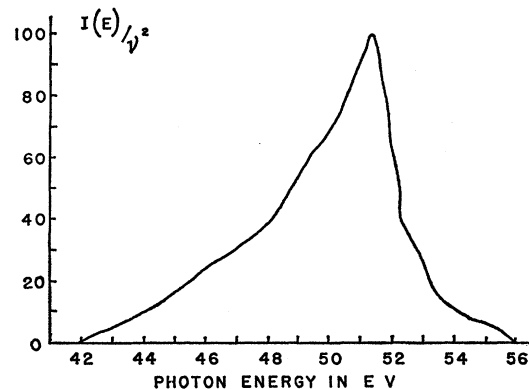


FIG. 2. The  $M_{2,3}$  emission band of iron. The ordinate represents the relative intensity  $I(E)$ , divided by the square of the radiated frequency  $\nu$  as a function of the energy  $E$  of the emitted photon.

<sup>4</sup> W. W. Beeman and H. Friedman, Phys. Rev. 56, 392 (1939).

<sup>5</sup> E. Gwinner, Z. Physik 108, 523 (1938).

The power radiated is given by

$$I_{a \rightarrow k} = h\nu_{a \rightarrow k} n_a \dot{n}_{a \rightarrow k} = h\nu_{a \rightarrow k} n_a P_{a \rightarrow k}^R / P_a,$$

in which  $\nu_{a \rightarrow k}$  is the radiated frequency. The de-ionization of the excited state is brought about by a radiative process as well as an Auger reorganization of the atom. If  $P_a^R$  and  $P_a^A$  are, respectively, the total transition probabilities per sec for the radiative and Auger processes, then  $P_a = P_a^R + P_a^A$  provided the two processes are independent. Then, the expression

$$I_{a \rightarrow k} = h\nu_{a \rightarrow k} n_a P_a^R / (P_a^R + P_a^A) = h\nu_{a \rightarrow k} n_a \omega_{a \rightarrow k}$$

indicates, in a formal way, the influence of the Auger de-ionization upon the intensity of the emission line. The quantity  $\omega_{a \rightarrow k}$  appearing in the last equation is the fluorescent yield of the emitted line.

To simulate the case of the  $M_3$  and  $M_2$  levels we need to compare the relative intensities of lines which originate from different excited states  $M_3$  and  $M_2$  (here denoted by  $a$  and  $b$ ) and have a common final state  $k$  corresponding to a hole in the conduction band. For this purpose we first write an expression for  $I_{b \rightarrow k}$  and then obtain the intensity ratio

$$I_{a \rightarrow k} / I_{b \rightarrow k} = (\nu_{a \rightarrow k} / \nu_{b \rightarrow k}) (n_a / n_b) (\omega_{a \rightarrow k} / \omega_{b \rightarrow k}).$$

For the case of the  $M_3$  and  $M_2$ , the ratio of the radiated frequencies is nearly equal to unity and the ratio of the rates of creation of vacancies may be taken equal to the ratio of  $(2J+1)_{M_3} / (2J+1)_{M_2}$  which is equal to 2. There is practically no information<sup>6</sup> on the fluorescent yields for  $M$  spectra but the yield is expected to be small. However, because of the relatively greater de-ionization of the  $M_2$  state by a radiationless transition, the  $(\omega_{a \rightarrow k}) / (\omega_{b \rightarrow k})$  ratio will be greater than unity. Hence, the  $M_3 / M_2$  intensity ratio must be greater than 2.

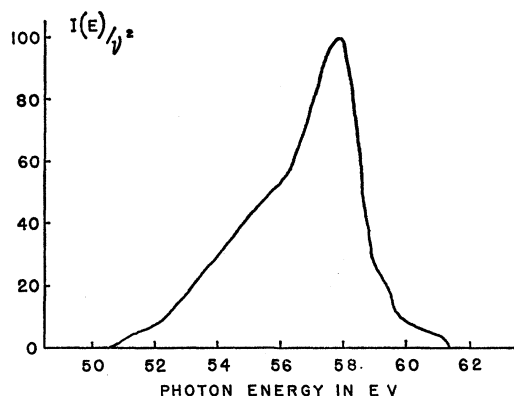


FIG. 3. The  $M_{2,3}$  emission band of cobalt. The ordinate represents the relative intensity  $I(E)$ , divided by the square of the radiated frequency  $\nu$  as a function of the energy  $E$  of the emitted photon.

<sup>6</sup> E. H. S. Burhop, *The Auger Effect* (Cambridge University Press, New York, 1952).

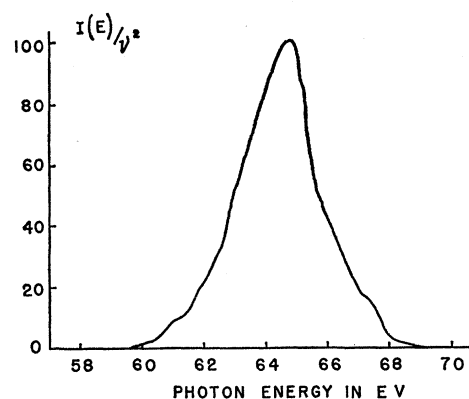


FIG. 4. The  $M_{2,3}$  emission band of nickel. The ordinate represents the relative intensity  $I(E)$ , divided by the square of the radiated frequency  $\nu$  as a function of the energy  $E$  of the emitted photon.

An attempt to obtain the individual  $M_2$  and  $M_3$  emission bands was undertaken in the case of the iron spectrum first by fixing the inner level separation at 1.5 eV and then by assigning reasonable values to the  $M_3 / M_2$  intensity ratio. The adopted value of the  $(M_2 - M_3)$  separation receives support from earlier observations<sup>7</sup> of  $M_{2,3}$  emission spectra and is not in conflict with a resolution of the observed  $M_{2,3}$  absorption curve of iron.<sup>8</sup>

In decomposing the observed curve for iron,  $M_3 / M_2$  intensity ratios of 2, 3, and 4 were tried in succession. Most realistic results were attained when the value of 3 was chosen for this ratio. A resolution of this type is not very sensitive to small changes in the adopted value of  $(M_2 / M_3)$  separation. However, when the intensity ratio was taken as 2 (this is the value predicted solely on the basis of the statistical weights) and again when the value was set equal to 4, the individual curves did show definite inconsistencies. In the actual carrying out of the separation, the general scheme described in reference 1 was followed.

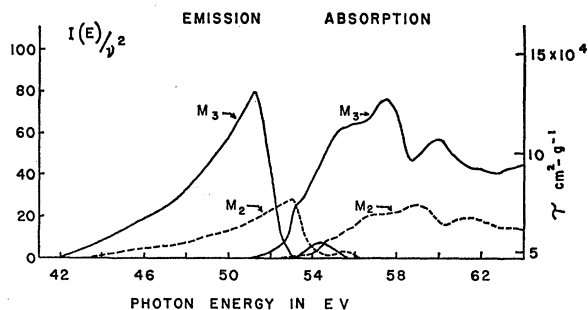


FIG. 5. A resolution of the observed  $M_{2,3}$  emission and absorption spectra of iron into individual  $M_2$  (dashed line) and  $M_3$  (solid line) emission and absorption curves.

<sup>7</sup> H. W. B. Skinner, T. G. Bullen, and J. E. Johnston, *Phil. Mag.* **45**, 1070 (1954).

<sup>8</sup> D. H. Tomboulion, D. E. Bedo, and W. M. Neupert, *J. Phys. Chem. Solids* **3**, 282 (1957).

The individual  $M_2$  and  $M_3$  emission curves for iron resulting from this process of decomposition are shown in the plot of Fig. 5. A satellite structure is clearly observable at the high-energy band edge. The individual bands may be isolated approximately from the influence of the low-energy tail and the satellite structure by extrapolating the more rapidly decaying portion of the profile until it intersects the energy axis. Following this procedure, the  $M_3$  and  $M_2$  edges are located at 53.0 and 54.5 ev and the bandwidth is estimated to be 8.0 ev.

The results of absorption measurements<sup>8</sup> carried out earlier with the same energy calibration are also included in Fig. 5. The individual absorption curves were deduced by a procedure resembling the one used in decomposing the emission band. However, for the reason given below, the  $M_3/M_2$  ratio of absorption coefficients was taken equal to two.

In the initial state of the absorption process the atom is in its ground state. Upon the absorption of a photon of appropriate energy, the atom is ionized in one of the inner shells. Thus, the absorption transitions start from a common level of low energy and end on different excited states, for instance the  $M_3$  or  $M_2$  states. The absorption coefficient  $\mu_{k \rightarrow a}$  corresponding to a transition from state  $k$  to a state  $a$  of higher energy, is equal to the power absorbed from the incident beam by the number of atoms per unit volume divided by the beam intensity.<sup>8</sup> Accordingly

$$\mu_{k \rightarrow a} \sim N_a P_{k \rightarrow a} h\nu_{k \rightarrow a},$$

where  $N_a$  is the total number of atoms per unit volume which may be excited by the ejection of a photoelectron from a state  $a$ ,  $P_{k \rightarrow a}$  is the absorption probability per unit time, and  $h\nu_{k \rightarrow a}$  is the energy of the absorbed photon. Upon comparing the absorption coefficients  $\mu_{k \rightarrow a}$  and  $\mu_{k \rightarrow b}$  corresponding to two transitions originating from a common state  $k$ , we obtain

$$\mu_{k \rightarrow a} / \mu_{k \rightarrow b} = (P_{k \rightarrow a} / P_{k \rightarrow b}) (\nu_{k \rightarrow a} / \nu_{k \rightarrow b}) \times [(2J+1)_a / (2J+1)_b],$$

where the statistical weights have been introduced to take into account the degeneracy of states  $a$  and  $b$ . Since the energies of the absorbed photons and the transition probabilities are nearly the same, the ratio  $\mu_{k \rightarrow a} / \mu_{k \rightarrow b} = 2$  if the states  $a$  and  $b$  are identified with the  $M_3$  and  $M_2$  levels for which  $J = \frac{3}{2}$  and  $J = \frac{1}{2}$ , respectively. In a more complete consideration of the absorption process, one must include the lifetime of the states  $a$  and  $b$ . A treatment of this sort will influence the shape of the absorption curve in the vicinity of the edge and thereby alter the numerical value of the ratio of absorption coefficients as deduced for the case of sharp levels.

The decomposed absorption curves are also plotted in Fig. 5. A comparison of the absorption and emission curves indicates that the onset of  $M_3$  absorption at 53.0 ev coincides with the high-energy limit of the  $M_3$

emission band. A similar agreement is found in the case of the  $M_2$  emission and absorption edges.

Because of the somewhat artificial nature of the procedure, no attempt was made to resolve the  $M_{2,3}$  bands of cobalt and nickel. A comparison of the location of the emission edges of the composite spectra is consistent with the corresponding data<sup>8</sup> on absorption edges. When more reliable information becomes available with regard to the  $(M_2-M_3)$  interval and with regard to  $M_3/M_2$  intensity ratios perhaps a unique resolution will be possible.

## DISCUSSION

The iron and nickel valence  $\rightarrow 3p$  bands have been examined by Gyorgy and Harvey<sup>9</sup> who used electronic detection schemes and recorded rates of photon emission from targets with a low power input (700 volts and 3 ma). The metal under study was deposited on the target continuously. Photometric determination of the  $M_{2,3}$  bands of the  $3d$  transition metals was carried out by Skinner *et al.*<sup>7</sup> under experimental conditions which simulated those prevailing in the present measurements. For the purpose of comparison, appropriate conversions were applied to these earlier observations. Unfortunately the previous information was available only in graphical form so that small inaccuracies are introduced in the process of transcription. The existing data on the  $M_{2,3}$  emission bands of the ferromagnetic metals appear in the graphs of Figs. 6, 7, and 8.

As indicated these results were obtained under different experimental conditions, and different techniques were utilized for measuring relative intensities. Variations in the observed shapes may originate from the presence of contaminants, differing physical states of aggregation of the photon emitting layer, self-absorption in the target, the procedure followed in removing the background, and a variety of instrumental effects

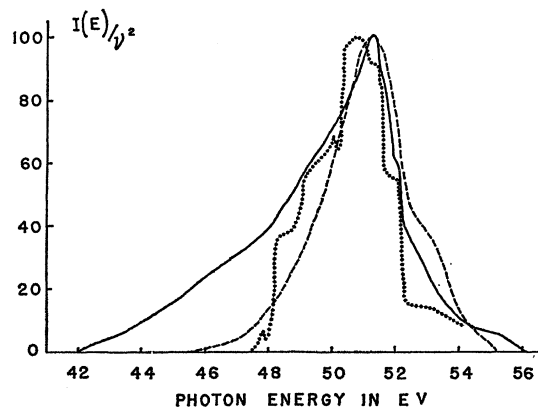


Fig. 6. A comparison of the existing data on the  $M_{2,3}$  emission band of iron. — Present measurements; ---- data from reference 7; .... data from reference 9.

<sup>9</sup> E. M. Gyorgy and G. G. Harvey, Phys. Rev. 93, 365 (1954).

such as resolving power and the establishment of the energy scale.

The three sets of measurements agree rather well as to the position of the peak. However, there are differences in the profiles. The photometric measurements seem to show greater repeatability, the main difference in the results deduced by this scheme of detection, arises from the procedure followed in removing the continuum intensity. The decision made with regard to the background contribution determines sensitively what the bandwidth shall be. It is believed that the procedure followed in the present measurements is considerably more reliable. The spectral distributions obtained by the photon-counting technique give rise to bands which are narrower and show abrupt intensity

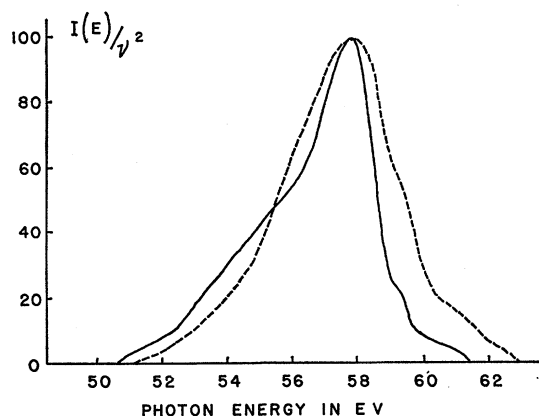


FIG. 7. A comparison of the existing data on the  $M_{2,3}$  emission band of cobalt. — Present measurements; ---- data from reference 7.

variations. It is conceivable that these observations arise from the nature of the target deposit and the shallower penetration of bombarding electrons. When low-voltage electrons are used, the photons are produced at depths which are likely to be a quasi-crystalline conglomerate of atoms and the sampling is from a region which is not characteristic of the normal periodicity.

There are really no sharp emission edges. Part of the observed edge diffuseness arises from the blending brought about by satellite structure. The bands show evidence of "tailing" towards long wavelengths.

Since a common energy scale was used in obtaining the present emission and absorption curves, the relative positions of such curves can be established quite accurately, to within 0.1 eV. There is some overlap between

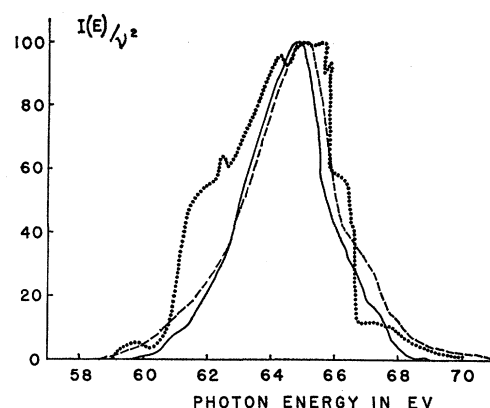


FIG. 8. A comparison of the existing data on the  $M_{2,3}$  emission band of nickel. — Present measurements, ---- data from reference 7; .... data from reference 9.

the two sets of curves, since the  $M$  levels are expected to have widths of several tenths of eV.

It is a common assumption that the transition probabilities are independent of the energy over the width of the band. Thus the intensity measurements should reflect a combined effect of  $N(E)|_{4s}$  and  $N(E)|_{3d}$ , the  $4s$  and  $3d$  contributions to the  $N(E)$  density of states curve. For the iron group of metals  $N(E)|_{4s}$  is expected to be a wide distribution with low density of states, whereas  $N(E)|_{3d}$  may be presumed to be narrower and higher.

A density of states curve for nickel obtained recently by Koster<sup>10</sup> shows again a pronounced dip in the  $3d$  band level density. This feature has been predicted by many previous calculations of the band structure. The experimental observations reported here show no evidence for a splitting of the  $3d$  band.

Wood<sup>11</sup> has recently examined the character of one-electron wave functions for the  $d$  band of body-centered iron. Although he has not obtained an accurate density of states curve for the  $3d$  band structure, his analysis indicates that there are five  $3d$  electron states per atom below an energy of 0.7 rydberg. Although the position of the Fermi level is not specified, the above description would perhaps imply that the filled  $(4s+3d)$  band in iron may be 6 eV–8 eV wide.

#### ACKNOWLEDGMENT

The authors take this opportunity to thank Dr. Richard D. Deslattes for many helpful discussions.

<sup>10</sup> G. F. Koster, Phys. Rev. **98**, 901 (1955).

<sup>11</sup> J. H. Wood, Phys. Rev. **117**, 714 (1960).